

ESO Phase 3 Data Release Description

Data Collection	VVV_CAT
Release Number	1
Data Provider	D. Minniti, P. Lucas and the VVV team
Date	27.11.2013

Abstract

The VVV Survey data delivered in this part of ESO Data Release 1 (DR1) includes the VISTA/VIRCAM paw-print and tile images that were acquired until September 30, 2010, and processed by the Cambridge Astronomical Survey Unit (CASU). This “VVV_CAT” data release contains the single-epoch band-merged (Z,Y,J,H,Ks) catalogues associated with the VVV tile images that have already been released in the part of DR1 identified as “VVV” in the ESO archive. VVV_CAT contains 269 tile catalogues.

Overview of Observations

The VVV photometry is divided into different disk and bulge tiles. The tile nomenclature goes from d001 to d152 in the disk, and from b201 to b396 in the bulge. The map with the field IDs is shown in Figures 1a and 1b, overlapped on the extinction map of the inner Milky Way from Schlegel et al. 1997.

The J,H and Ks images for each tile were obtained contemporaneously within a single OB, so that the time interval between images in different filters does not exceed 20 minutes. The Z and Y images for each tile were grouped together in another OB, separate from the JHKs OBs.



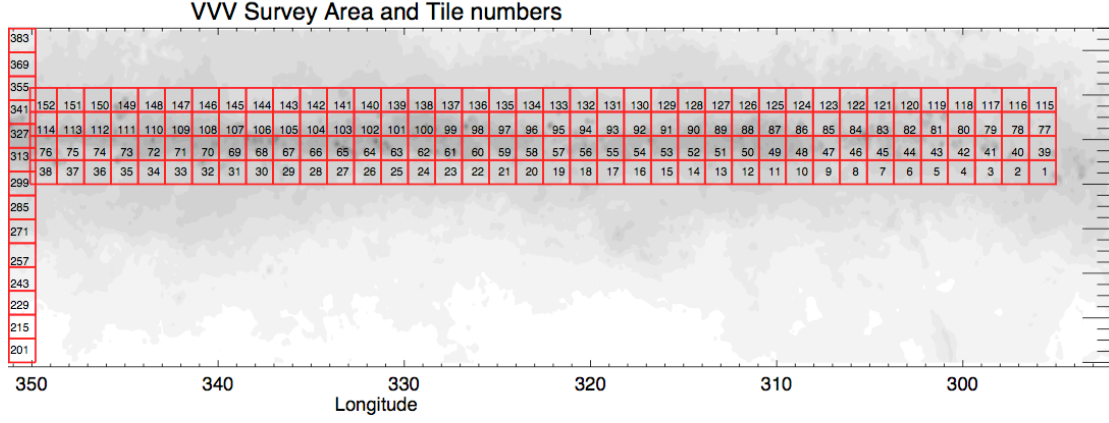


Figure 1. Maps showing the VVV tile numbers for: (a) bulge (upper panel); and (b) disk (lower panel).

Release Content

The VVV Survey observations planned for Year 1 (ESO Period 85) comprised JHKs maps as first priority, ZY maps as second priority, and 5 epochs in the Ks-band to test for variability, for the entire bulge and disk fields (all 348 tiles covering >520 sqdeg).

The VVV Survey Year 1 data completion is illustrated in Figures 2-3. The files for this VVV Survey DR1 include images and their respective photometric catalogues that have passed the Quality Control (QC), i.e. not all the fields shown in Figures 2-4 are being included in DR1, only higher quality data. For the Phase 3 DR1 of Year 1 we defined the list of data files that pass all the quality and calibration checks in order to be released, and at the same time defined a list of deprecated images, or re-reduced/re-calibrated some acceptable files.

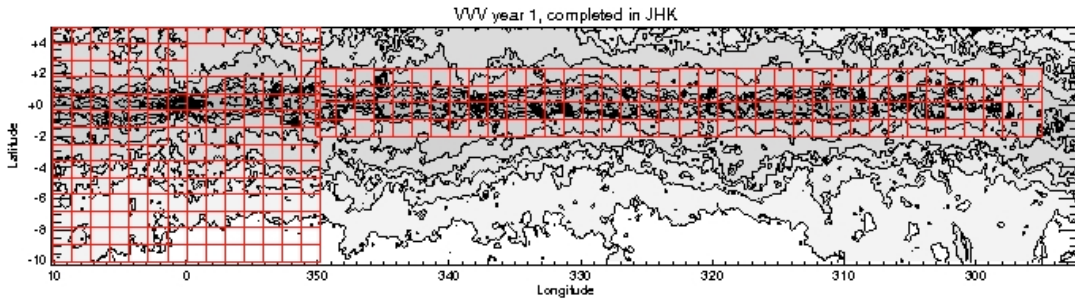


Fig. 2. VVV Survey observations completed in JHKs until Oct 1st, 2010. These OBs were given the highest priority, and the multicolor map of the VVV survey region is almost complete.

There are still observations pending from YEAR 1, as shown below in the maps of ZY filter observations (credit M. Hempel). These show **completed** tiles, but there

are still pending observations. In addition to the two YZ maps, the map of JHKs is mostly completed, but with 20 tiles still queued for observations.

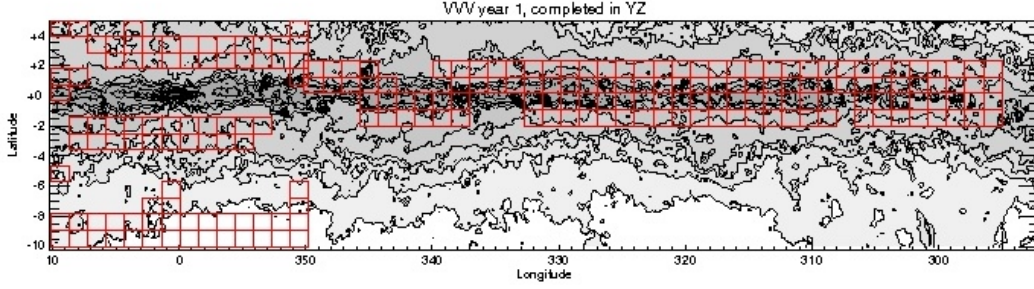


Fig. 3. VVV Survey observations completed in ZY until Oct 1st, 2010. These ZY filter observations were given slightly lower priority than the JHKs maps. However, we obtained significant coverage, specially in the disk region. These filters are essential to complement and interpret the information provided by the JHKs maps: they can lift the degeneracy or ambiguity of the JHKs color-color diagrams and color-magnitude diagram in the presence of large and variable interstellar extinction.

Sources were band-merged using a matching radius of 1 arcsec. The coordinates given in the catalogues are an average of the coordinates in each passband, weighted according to the errors. In total, the catalogues contain 2.08×10^8 sources, although about 10% of these are duplicate detections because of the overlaps between adjacent tiles. Catalogues in the disk region are deeper than the bulge region, owing to longer integration times and less source confusion. The 5 sigma photometric limits for isolated sources in the disk region are typically $Z=20.5$, $Y=20.0$, $J=19.5$, $H=19.0$, $Ks=18.0$. In the bulge region the limits vary widely, so it is not useful to quote a single figure for each passband. Note that the quoted errors do not take account of blending between adjacent sources, although the aperture photometry does deblend the fluxes in adjacent overlapping apertures. The “pperrbits” parameter for each passband indicates whether a given magnitude may be unreliable. The pperrbits numbers are additive, to allow for the possibility of more than one problem for an entry. The values in use here are: 16 (source has been deblended), 64 (a bad pixel exists in the default 2 arcsec diameter aperture), 32768 (source lies in a poor flat field region), 65536 (source is saturated, or close to saturation), 131072 (photometric calibration problem), 4191304 (source lies within a dither offset of the tile boundary). E.g. “zpperrbits=16” indicates that deblending of adjacent sources has been used when calculating the given magnitude in the Z passband. In general pperrbits values below 256 indicates no serious issues. Saturated stars usually have erroneous magnitudes, as indicated by pperrbits values of 65536 or higher.

Release Notes

Data Reduction and Calibration

The pipeline is composed of the following main steps: reset correction, dark

current subtraction, linearity correction, flat field correction, sky background correction, de-stripping (removal of a consistent electronic signal pattern from the arrays), illumination correction, image stacking into tiles, catalogue generation and then astrometric and photometric calibration. The sky background correction is based on the combination of 24 distinct VISTA pointings over 2 consecutive tiles imaged in the same OB, which has proven to be sufficient to remove stars in crowded VVV fields.)

The following procedures are done on an individual tile basis. The photometric calibration on to the VIRCAM (Vega-based) photometric system is derived from the 2MASS Point Source Catalogue, using relatively blue 2MASS sources with JHKs detections with <0.1 mag uncertainties in all 3 passbands, $0 < (J-K_s) < 2$ (as observed in 2MASS) and $0 < (J-K_s)_0 < 1$ (after dereddening the 2MASS sources individually using a prescription involving the Schlegel COBE/DIRBE extinction maps. Linear transformations between the 2MASS and VIRCAM photometric systems were applied that incorporate a colour term (based on 2MASS colours) and an extinction term based on the Schlegel maps). Aperture corrections are different for the 96 different sections of each VIRCAM tile (made from 6 pointings of the 16 arrays) and this is accounted for in the calibration after generation of the tiles and construction of initial tile catalogues.

An overlap analysis between adjacent tiles was used to confirm that nearly all tiles have consistent calibrations, though further small improvements are being made as the pipeline is continuously improved.

Aperture-corrected source magnitudes are provided in 3 concentric apertures: *apermag1* (1 arcsec diameter), *apermag3* (2 arcsec diameter), *apermag4* ($2\sqrt{2}$ arcsec diameter). *Apermag1* is most reliable for blended sources in crowded fields, whereas *apermag3* and *apermag4* benefit from more reliable aperture corrections.

The astrometric calibration is relative to the 2MASS Point Source Catalogue, with a typical precision of 0.08 arcsec for bright isolated stars.

Source detection requires 4 contiguous simply-connected pixels to be above a detection threshold set at 1.5 times the r.m.s. sky noise. Prior to source detection, the tile images are spatially filtered to remove the pattern of joins between the 96 components sections of a tile using a ~ 30 arcsec spatial filter. Nebulosity on smaller scales (e.g. in star formation regions) is not removed and this can affect detection and photometry of faint stars. Note that the spatial filter was not used on the tile images in the “VVV” data collection, only from the images used for source detection.

Quality Control

The DR1 is based on version v1.1 of the data reduction pipeline developed by the Cambridge Astronomical Survey Unit (CASU).

Visual Quality Control was performed in different steps. The jpeg images of each tile were inspected to remove tiles with obvious defects, e.g. highly non-uniform background. Then, visual Quality control of VVV tiles was made on a fraction of the FITS images. A word of caution: this intense activity is continuing, and even though we checked the images for defects, we are still identifying images that need to be reprocessed or reacquired.

The Quality Control for the Phase 3 data from v1.1 was performed on the paw-prints with involvement of most of the scientists from the team. We checked image defects, telescope problems, seeing, zero points, magnitude limits, ellipticities, airmass, etc. There are a number of well known image defects intrinsic to VISTA, many of which are illustrated with pictures in the CASU and VVV web pages (document [vvv_defects.pdf](#)).

Algorithmic quality control cuts to remove images with low zero points (after correcting for the seasonal trend), seeing that was significantly outside specification, or high average ellipticity were also applied. These were based on the v1.0 reduction pipeline, but no significant changes are expected in the v1.1 data.

Known Issues

Users of the catalogues should be aware that ~1% of the area of each tile (at the top right, in pixel coordinates) suffers less reliable photometric calibration (particularly in the Z, Y and J passbands) owing to the poor quality of VISTA/VIRCAM detector no.16, whose quantum efficiency is highly variable in the upper part of the array. The region affected, any other regions of below average data quality in a given tile, can be seen by inspecting the confidence images in the “VVV” data collection.

Users should also note that the sections of each tile near the left and right edge (in pixel coordinates) have half the normal exposure time since they lie at the edge of the standard VISTA tiling pattern. These sections are each 0.092 degrees in width. Again, they can be seen by inspecting the confidence images in the “VVV” data collection.

Bright saturated stars produce local maxima around them which are interpreted as detections by the extraction software. These spurious objects are typically classified as extended and many of them have large ellipticities. In the bandmerged catalogue provided here they result in objects detected in only one band.

Saturated objects also have a "hole" in their centre visible as a dark spot in the images. This is due to the double correlated sampling used during image readout.

The completeness of the tile catalogues is good in the “disk” portion of the VVV survey but less good in the bulge, where source confusion is highest. This is discussed in detail in the VVV DR1 publication (Saito et al.2012).

Data Format

Files Types

There is only 1 type of file in this release: the band-merged multi-epoch tile catalogue FITS files.

Catalogue Columns

The formats are as follows. "A" = character string. "K"=64 bit integer. "D"=double precision. "E"= single precision. "I"=16 bit integer. "J"=32 bit integer.

IAUNAME; 29A; Unique identifier in IAU naming convention

sourceID; K; UID (unique over entire VSA via programme ID prefix) of this merged detection as assigned by merge algorithm

frameSetID; K; UID of the set of frames that this merged source comes from

ra2000; D; Celestial Right Ascension

. RA and Dec are averaged across all bands, weighted by errors. The band-merging radius is 1 arcsec.

dec2000; D; Celestial Declination

l; D; Galactic longitude

b; D; Galactic latitude

lambda; D; SDSS system spherical co-ordinate 1

eta; D; SDSS system spherical co-ordinate 2

priOrSec; K; Seam code for a unique (=0) or duplicated (!=0) source (eg. flags overlap duplicates).

mergedClassStat; E; Merged $N(0,1)$ stellarness-of-profile statistic

mergedClass; I; Class flag from available measurements (1|0|-1|-2|-3|-9=galaxy|noise|stellar|probableStar|probableGalaxy|saturated)

zmyPnt; E; Point source colour Z-Y (using aperMag3)

zmyPntErr; E; Error on point source colour Z-Y

jmhPnt; E; Point source colour J-H (using aperMag3)

VVV DR1: The first data release of the Milky Way bulge and southern plane from the near-infrared ESO public survey VISTA variables in the Vía Láctea
jmhPntErr; E; Error on point source colour J-H

hmksPnt; E; Point source colour H-Ks (using aperMag3)

hmksPntErr; E; Error on point source colour H-Ks

zAperMag1; E; Extended source Z aperture corrected mag (0.7 arcsec aperture diameter)

zAperMag1Err; E; Error in extended source Z mag (0.7 arcsec aperture diameter)

zAperMag3; E; Default point/extended source Z aperture corrected mag (2.0 arcsec aperture diameter)

zAperMag3Err; E; Error in default point/extended source Z mag (2.0 arcsec aperture diameter)

zAperMag4; E; Extended source Z aperture corrected mag (2.8 arcsec aperture diameter)

zAperMag4Err; E; Error in extended source Z mag (2.8 arcsec aperture diameter)

zGausig; E; RMS of axes of ellipse fit in Z

zPA; E; ellipse fit celestial orientation in Z

zEll; E; $1-b/a$, where a/b =semi-major/minor axes in Z

zppErrBits; J; additional WFAU post-processing error bits in Z

.

zAverageConf; E; average confidence in 2 arcsec diameter default aperture (aper3) Z

zSeqNum; J; the running number of the Z detection

zXi; E; Offset of Z detection from master position (+east/-west)

zEta; E; Offset of Z detection from master position (+north/-south)

yAperMag1; E; Extended source Y aperture corrected mag (0.7 arcsec aperture diameter)

yAperMag1Err; E; Error in extended source Y mag (0.7 arcsec aperture diameter)

yAperMag3; E; Default point/extended source Y aperture corrected mag (2.0 arcsec aperture diameter)

yAperMag3Err; E; Error in default point/extended source Y mag (2.0 arcsec aperture diameter)

yAperMag4; E; Extended source Y aperture corrected mag (2.8 arcsec aperture diameter)

yAperMag4Err; E; Error in extended source Y mag (2.8 arcsec aperture diameter)

yGausig; E; RMS of axes of ellipse fit in Y

yPA; E; ellipse fit celestial orientation in Y

yEll; E; $1-b/a$, where a/b =semi-major/minor axes in Y

yppErrBits; J; additional WFAU post-processing error bits in Y

yAverageConf; E; average confidence in 2 arcsec diameter default aperture (aper3) Y

ySeqNum; J; the running number of the Y detection

yXi; E; Offset of Y detection from master position (+east/-west)

yEta; E; Offset of Y detection from master position (+north/-south)

jAperMag1; E; Extended source J aperture corrected mag (0.7 arcsec aperture diameter)

jAperMag1Err; E; Error in extended source J mag (0.7 arcsec aperture diameter)

jAperMag3; E; Default point/extended source J aperture corrected mag (2.0 arcsec aperture diameter)

jAperMag3Err; E; Error in default point/extended source J mag (2.0 arcsec aperture diameter)

jAperMag4; E; Extended source J aperture corrected mag (2.8 arcsec aperture diameter)

jAperMag4Err; E; Error in extended source J mag (2.8 arcsec aperture diameter)

jGausig; E; RMS of axes of ellipse fit in J

jPA; E; ellipse fit celestial orientation in J

jEll; E; $1-b/a$, where a/b =semi-major/minor axes in J

jppErrBits; J; additional WFAU post-processing error bits in J

jAverageConf; E; average confidence in 2 arcsec diameter default aperture (aper3) J

jSeqNum; J; the running number of the J detection

jXi; E; Offset of J detection from master position (+east/-west)

jEta; E; Offset of J detection from master position (+north/-south)

hAperMag1; E; Extended source H aperture corrected mag (0.7 arcsec aperture diameter)

hAperMag1Err; E; Error in extended source H mag (0.7 arcsec aperture diameter)

hAperMag3; E; Default point/extended source H aperture corrected mag (2.0 arcsec aperture diameter)

hAperMag3Err; E; Error in default point/extended source H mag (2.0 arcsec aperture diameter)

hAperMag4; E; Extended source H aperture corrected mag (2.8 arcsec aperture diameter)

hAperMag4Err; E; Error in extended source H mag (2.8 arcsec aperture diameter)

hGausig; E; RMS of axes of ellipse fit in H

hPA; E; ellipse fit celestial orientation in H

hEll; E; $1-b/a$, where a/b =semi-major/minor axes in H

hppErrBits; J; additional WFAU post-processing error bits in H

hAverageConf; E; average confidence in 2 arcsec diameter default aperture (aper3) H

hSeqNum; J; the running number of the H detection

hXi; E; Offset of H detection from master position (+east/-west)

hEta; E; Offset of H detection from master position (+north/-south)

ksAperMag1; E; Extended source Ks aperture corrected mag (0.7 arcsec aperture diameter)

ksAperMag1Err; E; Error in extended source Ks mag (0.7 arcsec aperture diameter)

ksAperMag3; E; Default point/extended source Ks aperture corrected mag (2.0 arcsec aperture diameter)

ksAperMag3Err; E; Error in default point/extended source Ks mag (2.0 arcsec aperture diameter)

ksAperMag4; E; Extended source Ks aperture corrected mag (2.8 arcsec aperture diameter)

ksAperMag4Err; E; Error in extended source Ks mag (2.8 arcsec aperture diameter)

ksGausig; E; RMS of axes of ellipse fit in Ks

ksPA; E; ellipse fit celestial orientation in Ks

ksEll; E; 1-b/a, where a/b=semi-major/minor axes in Ks

ksppErrBits; J; additional WFAU post-processing error bits in Ks

ksAverageConf; E; average confidence in 2 arcsec diameter default aperture (aper3) Ks

ksSeqNum; J; the running number of the Ks detection

ksXi; E; Offset of Ks detection from master position (+east/-west)

ksEta; E; Offset of Ks detection from master position (+north/-south)

VARFLAG; J; Classification of objects across all bands.

PRIMARY_SOURCE: The entries are derived from the priOrSec columns as follows:

PRIMARY_SOURCE = 1 IF (priOrSec=0 OR priOrSec=frameSetID)

PRIMARY_SOURCE = 0 otherwise

Acknowledgements

Credit: the VVV team. The References are:

D. Minniti, P. W. Lucas, J. P. Emerson, R. K. Saito, M. Hempel, P. Pietrukowicz, A. V. Ahumada, M. V. Alonso, J. Alonso-García, J. I. Arias, R. M. Bandyopadhyay, R. H. Barbá, L. R. Bedin, E. Bica, J. Borissova, L. Bronfman, M. Catelan, J. J. Clariá, N. Cross, R. de Grijs, I. Dékány, J. E. Drew, C. Fariña, C. Feinstein, E. Fernández Lajús, R. C. Gamen, D. Geisler, W. Gieren, B. Goldman, O. González, G. Gunthardt, S. Gurovich, N. C. Hambly, M. J. Irwin, V. D. Ivanov, A. Jordán, E. Kerins, K. Kinemuchi, R. Kurtev, M. López-Corredoira, T. Maccarone, N. Masetti, D. Merlo, M. Messineo, I. F. Mirabel, L. Monaco, L. Morelli, N. Padilla, M. C. Parisi, G. Pignata, M. Rejkuba, A. Roman-Lopes, S. E. Sale, M. R. Schreiber, A. C. Schröder, M. Smith, L. Sodr   Jr., M. Soto, M. Tamura, C. Tappert, M. A. Thompson, I. Toledo, M. Zoccali, “VISTA Variables in the Via Lactea (VVV): The public ESO near-IR variability survey of the Milky Way”, 2010, *New Astronomy*, 15, 433

R. K. Saito, M. Hempel, D. Minniti, P. W. Lucas, M. Rejkuba, I. Toledo, O. A. Gonzalez, J. Alonso-García, M. J. Irwin, E. Gonzalez-Solares, S. T. Hodgkin, J. R. Lewis, N. Cross, V. D. Ivanov, E. Kerins, J. P. Emerson, M. Soto, E. B. Am  res, S. Gurovich, I. Dékány, R. Angeloni, J. C. Beamin, M. Catelan, N. Padilla, M. Zoccali, P. Pietrukowicz, C. Moni Bidin, F. Mauro, D. Geisler, S. L. Folkes, S. E. Sale, J. Borissova, R. Kurtev, A. V. Ahumada, M. V. Alonso, A. Adamson, J. I. Arias, R. M. Bandyopadhyay, R. H. Barbá, B. Barbuy, G. L. Baume, L. R. Bedin, A. Bellini, R. Benjamin, E. Bica, C. Bonatto, L. Bronfman, G. Carraro, A. N. Chen  , J. J. Clari  , J. R. A. Clarke, C. Contreras, A. Corvill  n, R. de Grijs, B. Dias, J. E. Drew, C. Fari  a, C. Feinstein, E. Fern  ndez-Laj  s, R. C. Gamen, W. Gieren, B. Goldman, C. Gonz  lez-Fern  ndez, R. J. J. Grand, G. Gunthardt, N. C. Hambly, M. M. Hanson, K. G. Helminiak, M. G. Hoare, L. Huckvale, A. Jord  n, K. Kinemuchi, A. Longmore, M. L  pez-Corredoira, T. Maccarone, D. Majaess, E. L. Mart  n, N. Masetti, R. E. Mennickent, I. F. Mirabel, L. Monaco, L. Morelli, V. Motta, T. Palma, M. C. Parisi, Q. Parker, F. Pe  aloza, G. Pietrzy  ski, G. Pignata, B. Popescu, M. A. Read, A. Rojas, A. Roman-Lopes, M. T. Ruiz, I. Saviane, M. R. Schreiber, A. C. Schr  der, S. Sharma, M. D. Smith, L. Sodr   Jr., J. Stead, A. W. Stephens, M. Tamura, C. Tappert, M. A. Thompson, E. Valenti, L. Vanz  , N. A. Walton, W. Weidmann and A. Zijlstra, “VVV DR1: The first data release of the Milky Way bulge and southern plane from the near-infrared ESO public survey VISTA variables in the V  a L  ctea”, 2012, *A&A*, 537, A107

Please use the following statement in your articles when using these data:

Based on data products from observations made with ESO Telescopes at the La Silla Paranal Observatory under programme ID 179.B-2002.